Special Issue on Chemistry

Pedalium murex Plant Extract Assisted Synthesis and Antibacterial Properties of Fe$_2$(MoO$_4$)$_3$ Nanoparticles

R. Meera and K. Rajendran

CARAS

Full Length Research Article

Pedalium murex Plant Extract Assisted Synthesis and Antibacterial Properties of Fe$_2$(MoO$_4$)$_3$ Nanoparticles

R. Meera[1] and K. Rajendran*[2]

A B S T R A C T

Fe$_2$(MoO$_4$)$_3$ nanostructures are paying more attention owing to its tremendous usage in the catalytic activity such as removal of environmental pollutants and biomedical effect. In the present work, the novel Fe$_2$(MoO$_4$)$_3$ nanostructure synthesized by *Pedalium murex* plant extract assisted synthesis with heterogeneous assemblies was constructed and applied for the antibacterial agent of pathogens. The prepared heterostructure were examined by various analytical techniques like Powder XRD, FTIR, UV-DRS, PL, FESEM, HRTEM, EDX respectively. XRD pattern proved the crystallite size of various heterostructure were 27.91 nm respectively. Furthermore, the composite was examined as antibacterial agent and was found exhibit higher antibacterial efficiency against Klebsiellapneumoniae compared with other pathogens.

Key words: Antibacterial agent, Crystallite size, Catalytic activity, Nanocomposites, TiO$_2$

The enhancement of urbanization and industrialization is causing a lack of worldwide energy resources, food production, and a substantial amount of toxic pollutants is being released into the environment. Contemporary to overcome the demand of world food production, more attention has focused to achieve the high yield in agriculture. The constant development of world population needs to increase the consumption of plant growth and rise around 8 million in 2025 and 9 million in 2050 [1]. In global agriculture, the farmers used several pesticides to enhance the productivity and protect the crops from pests [2]. Pesticides are the organic substances used to kill the targeted pests like insects, fungus, microbes, mollusks and nematodes, which cause diseases in crops and effect on production [3]. Around the world 3.42×106 t/y number of pesticides was used in 2015 with the release of toxic effects to human, animals, micro-organism and pollute the environment [4]. Organophosphate (Ops) is the worldwide used pesticides and it restricts the enzyme acetyl cholinesterase (AChE). This enzyme is responsible for regular functioning of central nervous system in insects and humans, resulting paralysis, destroys respiratory organs finally leads to death [5]. Dichlorvos (2,2-dichlorovinyl dimethyl phosphate) is frequently used Ops in Indian agriculture to regulate the pests in fruits, vegetables, households also in storage of grains. According to U.S. Environmental Protection Agency considers as class I toxic to generate chronical diseases and cancer, hence it is banned to practice as

pesticide [6]. The detection of Ops is very important and has great interest in researchers. Many techniques are applied to detect the Organo pesticides for instance fluorescence sensor [7], amperometry, potentiometry, bio sensors [8], microbial biosensors, immunosensors, electrochemical sensors, conductometric detection, potentiometric detection, optical immunosensor, aptamers [9], square wave voltammetry (SWV) [10], differential pulse voltammetry (DPV), cyclic voltammetry [11] and HPLC [12]. Among this CV technique has paid more attention due to its high reliability, sensitivity, using simple instruments, easy to operate and getting immediate result [13].

In the past era, the increasing of world population, economies and developing countries are releases huge amount of toxic organic substances into water to destroy the ecosystem [14]. Per annum about 70,000 tonnes of untreated dyes with complex structures from various sectors such as textile, leather, pharmaceutical, paper, food and cosmetic industries are discharge around 1-15% of organic effluents in aquatic medium. It is least biodegradable also restrict penetration of sunlight into water bodies and spoil water ecosystem [15]. These organic pollutants have great impact on our daily life but due to fewer biodegradable natures, it causes some health hazards. Azo dyes are hard to degrade becomes extremely carcinogenic and genotoxic [16].

MATERIALS AND METHODS

Synthesis of Fe$_2$(MoO$_4$)$_3$

The Fe$_2$(MoO$_4$)$_3$ nano-powders have been synthesized with the aid of using the use of precursors consisting of 0.1 g of ferric nitrate and 0.02g of Ammonium molybdate was dissolved separately in 10 mL of distilled water in 100 mL beaker and *Pedalium murex* plant extract as a fuel that have been dissolved

* **K. Rajendran**
✉ rajendran1317@gmail.com

[1-2] Department of Chemistry, Bharath Institute of Higher Education and Research (BIHER), Chennai - 600 073, Tamil Nadu, India

CARAS

one at a time in 10 ml of deionized water and stirred for 15 minutes. Then it changed into located in a microwave-oven (2.forty five GHz, 750 W) for 10 minutes. Initially, the answer boiled and underwent dehydration observed with the aid of using decomposition with the evolution of gases. When the answer reached the factor of spontaneous combustion, it changed into vaporized and right away have become a strong and received with the aid of using MCM. When the solution reached the point of spontaneous combustion, it was vaporized and instantly became a solid.

Characterization of samples

As synthesized $Fe_2(MoO_4)_3$ samples were characterized using various analytical techniques. The phase purity and crystallite size were analysed by Powder XRD (PAN alytical X'PERT-PRO) X-ray diffractometer recorded at 40 kV and 30 mA with Cukα radiation (λ=1.5406 Aº) in the range 2θ=10º-70º under room temperature. Morphology was examined via Field emission scanning electron microscopy (FESEM, Hitachi S-3400) and High-resolution transmission electron microscopy (TEM/SAED) model EM-4101LS from Philips, Holland. Fourier transform infrared spectroscopy (FTIR) was recorded at Thermo Nicolet 380 spectrophotometer ranges 400-4000 cm-1 using standard KBr. The optical properties studied by emission spectra Varian Cary Eclipse (type: Svitzky-Golay) PL spectroscopy ranges 350-600 nm. UVDRS was recorded JASCOV650 spectrophotometer ranges 200-800 nm.

Antibacterial studies

The antibacterial activity of $Fe_2(MoO_4)_3$ nanostructure was examined by Agar well diffusion method. Three bacterial species Staphylococcus aureus, Escherichia coli and Pseudomonuas aeruginosa was chosen and taken in different concentration of samples. The preparation of bacterial culture was briefly explained in previous work [16]. 50, 25,12.5,6.25 and 1.125 mg/mL concentration of samples were dissolved in DMSO and poured into the well then, the plates were incubated at 37ºC for 24 hrs to achieve minimum zone of inhibition.

RESULTS AND DISCUSSION

Powder XRD analysis

The powder XRD studies of pure $Fe_2(MoO_4)_3$ nanostructure are shown in (Fig 1). Crystallite size and phase purity of the samples were determined via PXRD. (Fig 1) shows the PXRD pattern of $Fe_2(MoO_4)_3$, it displays the diffraction peaks at 2θ values of 25º, 17.49º, 30.15º, 45.71º, 56.08º are corresponds to planes (202), (121), (240), (122), (320) and cell parameters values of a=10.31, b=14.48 and c=9.749. These values are exactly match with JCPDCS CARD NO: 340101 of orthorhombic phase of $Fe_2(MoO_4)_3$. The absence of other impurity peaks in XRD pattern confirm the purity of the samples. Additionally, there is the strong electrostatic force of attraction takes place between the ions with different oxidation number and different planes in composites [17-19]. Moreover, the composites exhibit sharp intense peaks than the pure samples confirm the proper insertion of rare earth molybdates. The narrow peaks found in composites are evident for the formation of crystalline state. The phase purity, smaller in crystallite size and appropriate ratio of composite enhance the sample to be act as a good semi-conductor material in photocatalytic application.
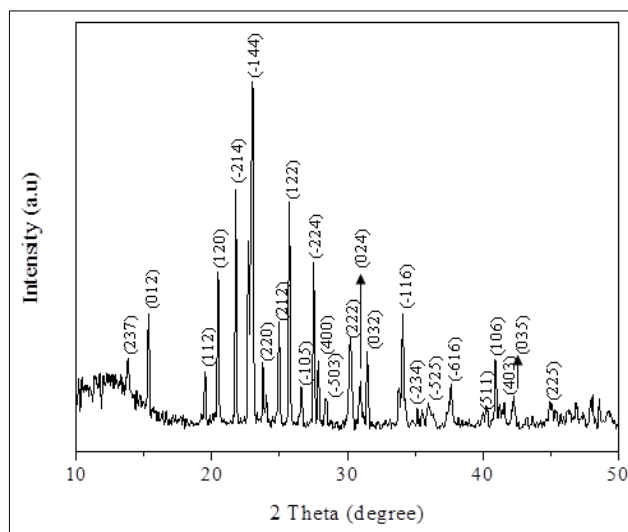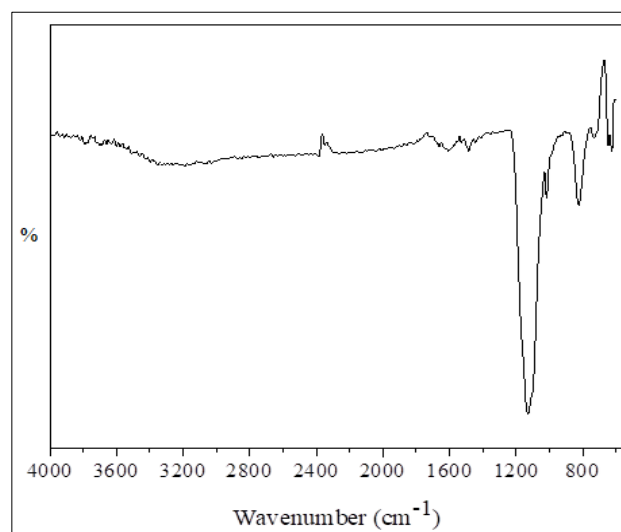

Fig 1 Powder XRD patterns of $Fe_2(MoO_4)_3$ NPs

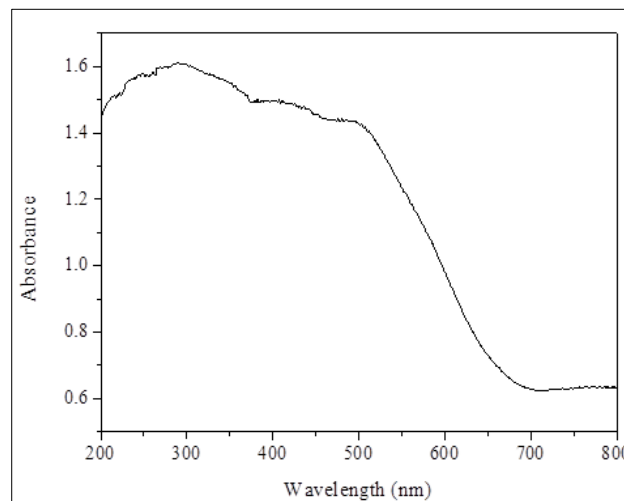Fig 2 FT-IR spectra of $Fe_2(MoO_4)_3$ NPs

FTIR spectrum

The structure of $Fe_2(MoO_4)_3$ nanoostructure at various concentrations was analyzed via FTIR spectrum shown in (Fig 2). It gives the detailed information about the types of bonds formed in the samples. In this spectrum the peaks found at 1609 cm-1 and above is corresponds to bending and stretching vibrations of water molecules [20,21]. The vibration bands around 965 cm-1 is dominated $Fe_2(MoO_4)_3$. Hence, the presence of molybdates in our samples are confirmed by this evidence. Although the strong bands near 824 and 778 cm-1 are attributed to Fe-O-Mo and Mo-O bands respectively confirm the formation of molybdates in composite materials. The presence of groups in FTIR spectrum confirms the formation of composites, hence it supports the PXRD results.

FESEM analysis

The surface morphology of $Fe_2(MoO_4)_3$ nanostructure was explored via FESEM technique at different magnification (Fig 3). The pure $Fe_2(MoO_4)_3$ sample exhibits potato like structure with high aggregation and porous in nature is observed in (Fig 3). This porosity increases the attraction of smaller particles and permits the movement of ions on its surface. This result nearly agrees with crystallite size calculated by PXRD method [22]. Additionally, the presence of different morphology is another evident for successful formation of composite; hence it is confirmed by existence of two phases in composites in XRD pattern. Thus, the binding nature and morphological changes are depending on calcination temperature and crystallite size also point out the absence of impurities.
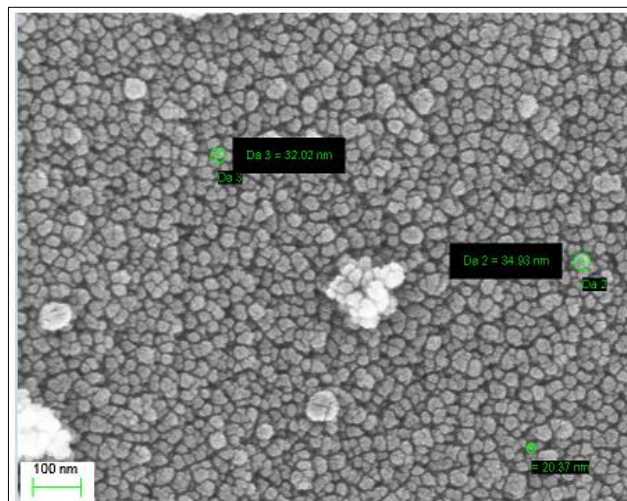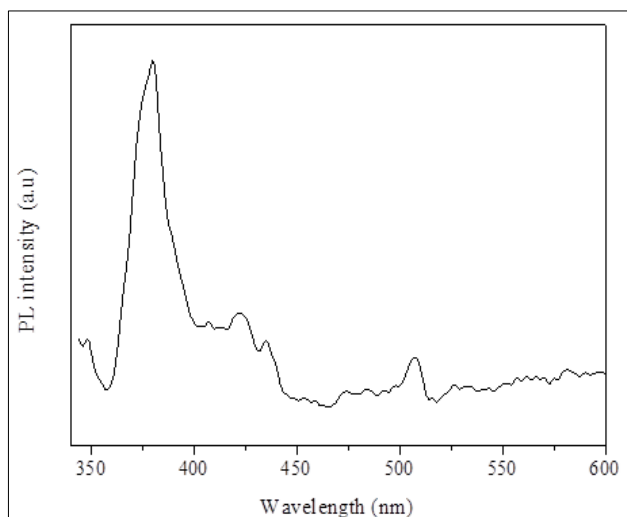
Fig 3 SEM images of $Fe_2(MoO_4)_3$ NPs

Fig 4 UV -DRS Spectroscopy of $Fe_2(MoO_4)_3$ NPs

UV -DRS Spectroscopy

The band gap energy of $Fe_2(MoO_4)_3$ nanostructure were determined by UV-Vis/DRS spectroscopy (Fig 4). The absorption spectra of titania are naturally change by addition of thorium molybdate, which enhance the absorption towards red shift region. Thus, the heterostructure can modify the level of CB and VB [20-25]. The reductions in band gap energy in composites are due to smaller in particle size, defects and morphology. The other observed results PXRD, FESEM and HRTEM confirm the unique property of this sample.
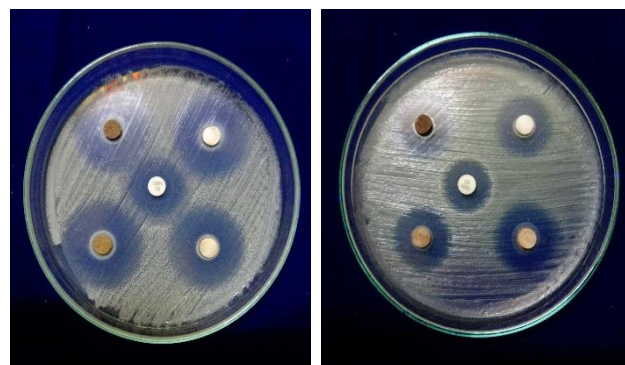
Photoluminescence spectroscopy (PL)

The study of surface states, electron transfer and recombination of electron-hole pairs are analyzed by PL spectroscopy. (Fig 5) shows emission spectra of $Fe_2(MoO_4)_3$ which gives detailed explanation about structural defect and sub-band gap defects. These defects can be change with crystallite size, morphology and reaction condition of the samples. The spectrum shows similar emission peaks for all samples at 360, 376, 411, 438, 490 and 518 nm respectively. The transition of electrons from higher to lower energy state is comparatively high in high crystalline sample. Likewise, lower in emission intensity is mainly depends on structural defects which can restrict the electron transition [24-30]. Above 530 nm the peaks slightly moves in the direction of red shift region indicates more oxygen vacancies which enhance the samples to act as a photocatalyst in visible light region.

Fig 5 Photoluminescence spectroscopy of $Fe_2(MoO_4)_3$ NPs

Fig 6 Antibacterial activity of $Fe_2(MoO_4)_3$ nanoparticles

Antibacterial activity

(Fig 6) shows the antibacterial activity of $Fe_2(MoO_4)_3$ NPs samples were investigated against gram negative (Klebsiellapneumoniae) and gram positive (Staphylococcus aureus) bacterial strains, respectively. From the images, it was found that there is no zone of inhibition over the control, which clearly shows that the zone of inhibition increases and influences higher antibacterial activity [35-39]. The particle size and surface area of the samples play a vital role in the antibacterial activity of synthesized samples.

CONCLUSION

$Fe_2(MoO_4)_3$ nanoostructure was successfully prepared by *Pedalium murex* plant extract assisted synthesis. Power XRD reveals the orthorhombic phase of $Fe_2(MoO_4)_3$. The crystallite sizes were estimated as 20.97 nm for $Fe_2(MoO_4)_3$. Optical studies states band gap energy was smaller for $Fe_2(MoO_4)_3$. The morphology of samples expresses potato like structure and cubic structure for $Fe_2(MoO_4)_3$. PL spectrum indicates the red shift due to oxygen vacancies enhance the photocatalyst in visible light region. It has been found that the $Fe_2(MoO_4)_3$ nanoparticles exhibit higher antibacterial efficiency against Klebsiellapneumoniae compared with other pathogens.

LITERATURE CITED

1. Murugan E, A Siva. 2005. Preparation of a novel soluble multi-site phase transfer catalyst and the kinetic study for the C-alkylation of α-pinene. *Journal of Molecular Catalysis A: Chemical* 235(1/2): 220-229.

2. Ratnayake SP, M Mantilaka, C Sandaruwan, D Dahanayake, E Murugan. 2019. Carbon quantum dots-decorated nano-zirconia: a highly efficient photocatalyst. *Applied Catalysis A: General* 570: 23-30.

3. Murugan E, P Gopinath, V Shanmugayya, N Mathivanan. 2010. Antibacterial activity of novel insoluble bead-shaped polymer-supported multiquaternary ammonium salts, *Journal of Applied Polymer Science* 117(6): 3673-3678.

4. Murugan E, I Pakrudheen. 2015. Efficient amphiphilic poly (propylene imine) dendrimer encapsulated ruthenium nanoparticles for sensing and catalysis applications. *Science of Advanced Materials* 7(5): 891-901.

5. Murugan E, JN Jebaranjitham, Usha A. 2012. Synthesis of polymer-supported dendritic palladium nanoparticle catalysts for Suzuki coupling reaction. *Applied Nanoscience* 2(3): 211-222.

6. Murugan E, JN Jebaranjitham, KJ Raman, A Mandal, D Geethalakshmi. 2017. Insoluble dendrimer-grafted poly (vinylimidazole) microbeads stabilized with mono/bimetallic nanoparticle catalysts for effective degradation of malachite green. *New Journal of Chemistry* 41(19): 10860-10871.

7. Murugan E, SS Kumar, KM Reshna, S Govindaraju. 2019. Highly sensitive, stable g-CN decorated with AgNPs for SERS sensing of toluidine blue and catalytic reduction of crystal violet. *Journal of Materials Science* 54(7): 5294-5310.

8. Murugan, M Ariraman, S Rajendran, J Kathirvel, CR Akshata, K Kumar. 2018. Core–Shell Nanostructured Fe_3O_4–Poly(styrene-co-vinylbenzyl chloride) Grafted PPI Dendrimers Stabilized with AuNPs/PdNPs for Efficient Nuclease Activity. *ACS Omega* 3(10): 13685-13693.

9. Shanmugam P, K Rajakumar, R Boddula, RC Ngullie, W Wei, Xie J. 2019. Heterogeneous form of poly (4-vinyl pyridine) beads based dendrimer stabilized Ag, Au and PdNPs catalyst for reduction of trypan blue. *Materials Science for Energy Technologies* 2(3): 532-542.

10. Murugan E, S Santhoshkumar, S Govindaraju, Palanichamy M. 2021. Silver nanoparticles decorated g-C3N4: An efficient SERS substrate for monitoring catalytic reduction and selective Hg2+ ions detection. *Spectrochimica Acta Part A: Molecular and Biomolecular Spectroscopy* 246: 119036.

11. Santhoshkumar S, Murugan E. 2021. Rationally designed SERS AgNPs/GO/g-CN nanohybrids to detect methylene blue and Hg2+ ions in aqueous solution. *Applied Surface Science* 553: 149544.

12. Ratnayake SP, C Sandaruwan, M Mantilaka, N de Silva, D Dahanayake, U.K Wanninayaka, W.R.L.N. Bandara, S. Santhoshkumar, E. Murugan, G.A.J. Amaratunga, K.M. Nalinde Silv. 2021. Industrial and environmental significance of photonic zirconia nanoflakes: Influence of boron doping on structure and band states. *Journal of Industrial and Engineering Chemistry* 95: 203-214.

13. Pakrudheen I, AN Banu, Murugan E. 2018. Cationic amphiphilic dendrimers with tunable hydrophobicity show in vitro Activity. *Environmental Chemistry Letters* 16(4): 1513-1519

14. Murugan E, A Rubavathy Jaya Priya, K Janaki Raman, K Kalpana, C R Akshata, S Santhoshkumar, Govindaraju S. 2019. Multiwalled carbon nanotubes/gold nanoparticles hybrid electrodes for enzyme-free electrochemical glucose sensor. *Journal of Nanoscience and Nanotechnology* 19(12): 7596-7604

15. Murugan E, Rangasamy R. 2011. Development of stable pollution free TiO2/Au nanoparticle immobilized green photo catalyst for degradation of methyl orange. *Journal of Biomedical Nanotechnology* 7(1): 225-228.

16. Murugan E, Vimala G. 2013. Synthesis, characterization, and catalytic activity for hybrids of multi-walled carbon nanotube and amphiphilic poly(propyleneimine) dendrimer immobilized with silver and palladium nanoparticle. *Journal of Colloid and Interface Science* 396: 101-111.

17. Murugan E, Vimala G. 2011. Effective functionalization of multiwalled carbon nanotube with amphiphilic poly(propyleneimine) dendrimer carrying silver nanoparticles for better dispersability and antimicrobial activity. *Journal of Colloid and Interface Science* 357(2): 354-365.

18. Murugan E, Jebaranjitham JN. 2015. Dendrimer grafted core–shell Fe_3O_4–polymer magnetic nanocomposites stabilized with AuNPs for enhanced catalytic degradation of Rhodamine B–A kinetic study. *Chemical Engineering Journal* 259: 266-276.

19. Murugan E, Gopi V. 2011. Amphiphilic multiwalled carbon nanotube polymer hybrid with improved conductivity and dispersibility produced by functionalization with poly (vinylbenzyl) triethylammonium chloride. *The Journal of Physical Chemistry C* 115(40): 19897-19909.

20. Murugan E, RL Sherman, Spivey HO. 2004. Catalysis by hydrophobically modified poly (propylenimine) dendrimers having quaternary ammonium and tertiary amine functionality. *WT Ford, Langmuir* 20(19): 8307-8312.

21. Manikandan A, M. Durka, Arul S. 2015. Antony, magnetically recyclable spinel $Mn_xZn_{1-x}Fe_2O_4$; $(0.0 \leq x \leq 0.5)$ nano-photocatalysts. *Advanced Science, Engineering and Medicine* 7: 33-46.

22. Manikandan A, A. Saravanan, S. Arul Antony, Bououdina M. 2015. One-pot low temperature synthesis and characterization studies of nanocrystalline α-Fe_2O_3 based dye sensitized solar cells. *Journal of Nanoscience and Nanotechnology* 15: 4358-4366.

23. Valan MF, A. Manikandan, Antony SA. 2015. A novel synthesis and characterization studies of magnetic Co_3O_4 nanoparticles. *Journal of Nanoscience and Nanotechnology* 15: 4580-4586.

24. Valan MF, A. Manikandan, Antony SA. 2015. Microwave combustion synthesis and characterization studies of magnetic $Zn_{1-x}Cd_xFe_2O_4$ $(0 \leq x \leq 0.5)$ nanoparticles. *Journal of Nanoscience and Nanotechnology* 15: 4543-4551.

25. Jayasree S, A. Manikandan, A. M. *Uduman Mohideen*, C. Barathiraja, Antony SA. 2015. Comparative study of combustion methods, opto-magnetic and catalytic properties of spinel $CoAl_2O_4$ nano- and microstructures. *Advanced Science, Engineering and Medicine* 7: 672-682.

26. Manikandan A, M. Durka, Antony SA. 2015. Hibiscus rosa-sinensis leaf extracted green methods, magneto-optical and catalytic properties of spinel $CuFe_2O_4$ nano- and microstructures. *Journal of Inorganic and Organometallic Polymers and Materials* 25: 1019-1031.

005

Res. Jr. of Agril. Sci. (Special) **13**: 001–005

27. Manikandan A, M. Durka, K. Seevakan, Antony SA. 2015. A novel one-pot combustion synthesis and opto-magnetic properties of magnetically separable spinel $Mn_xMg_{1-x}Fe_2O_4$ ($0.0 \leq x \leq 0.5$) nano-photocatalysts. *Journal of Superconductivity and Novel Magnetism* 28: 1405-1416.

28. Manikandan A, M. Durka, Antony SA. 2015. One-pot flash combustion synthesis, structural, morphological and opto-magnetic properties of spinel $Mn_xCo_{1-x}Al_2O_4$ ($x = 0$, 0.3 and 0.5) nano-catalysts. *Journal of Superconductivity and Novel Magnetism* 28: 209-218.

29. Manikandan A, E. Hema, M. Durka, K. Seevakan, T. Alagesan, Antony SA. 2015. Room temperature ferromagnetism of magnetically recyclable photocatalyst of $Cu_{1-x}Mn_xFe_2O_4$-TiO_2 ($0.0 \leq x \leq 0.5$) nano-composites. *Journal of Superconductivity and Novel Magnetism* 28: 1783-1795.

30. Manikandan A, M. Durka, Antony SA. 2015. Role of Mn^{2+} doping on structural, morphological and opto-magnetic properties of spinel $Mn_xCo_{1-x}Fe_2O_4$ ($x = 0.0$, 0.1, 0.2, 0.3, 0.4 and 0.5) nano-catalysts. *Journal of Superconductivity and Novel Magnetism* 28: 2047-2058.

31. Chinnaraj K, A. Manikandan, P. Ramu, S. Arul Antony, Neeraja P. 2015. Comparative study of microwave and sol-gel assisted combustion methods of Fe_3O_4 nanostructures: Structural, morphological, optical, magnetic and catalytic properties. *Journal of Superconductivity and Novel Magnetism* 28: 179-190.

32. Hema E, A. Manikandan, P. Karthika, M. Durka, Antony SA, Venkatraman BR. 2015. A novel synthesis of Zn^{2+}-doped $CoFe_2O_4$ spinel nanoparticles: Structural, morphological, opto-magnetic and catalytic properties. *Journal of Superconductivity and Novel Magnetism* 28: 2539-2552.

33. Manimegalai DK, A. Manikandan, S. Moortheswaran, Antony SA. 2015. Magneto-Optical and Photocatalytic Properties of Magnetically Recyclable $Zn_{1-x}Mn_xS$ ($x = 0.0$, 0.3 and 0.5) nano-catalysts. *Journal of Superconductivity and Novel Magnetism* 28: 2755-2766.

34. Umapathy V, A. Manikandan, S. Arul Antony, P. Ramu, Neeraja P. 2015. Synthesis, structural, morphological and opto-magnetic properties of Bi_2MoO_6 nano-photocatalyst by sol-gel method. *Transactions of Nonferrous Metals Society of China* 25: 3271-3278.

35. Sumithra V, A. Manikandan, M. Durka, S. K. Jaganathan, A. Dinesh, N. Ramalakshmi, Antony SA. 2017. Simple precipitation synthesis, characterization and antibacterial activity of Mn-doped ZnO nanoparticles. *Advanced Science, Engineering and Medicine* 9: 483-488.

36. Bomila R, S. Srinivasan, S. Gunasekaran, Manikandan A. 2018. Enhanced photocatalytic degradation of methylene blue dye, opto-magnetic and antibacterial behaviour of pure and La-doped ZnO nanoparticles. *Journal of Superconductivity and Novel Magnetism* 31: 855-864.

37. Elayakumar K, A. Dinesh, A. Manikandan, P. Murugesan, G. Kavitha, S. Prakash, R. T. Kumar, S. K. Jaganathan, Baykal A. 2019. Structural, morphological, enhanced magnetic properties and antibacterial bio-medical activity of rare earth element (REE) Cerium (Ce^{3+}) doped $CoFe_2O_4$ nanoparticles. *Journal of Magnetism and Magnetic Materials* 476: 157-165.

38. Ravichandran AT, J. Srinivas, A. Manikandan, Baykal A. 2019. Enhanced magneto-optical and antibacterial studies of $Bi_{1-x}Mg_xFeO_3$ ($0.0 \leq x \leq 0.15$)) nanoparticles. *Journal of Superconductivity and Novel Magnetism* 32: 1663-1670.

39. Babitha N, L. Srimathi Priya, S. Rosy Christy, A. Manikandan, A. Dinesh, M. Durka, Arunadevi S. 2019. Enhanced Antibacterial Activity and Photo-Catalytic Properties of ZnO Nanoparticles: *Pedalium Murex* Plant Extract-Assisted Synthesis. *Journal of Nanoscience and Nanotechnology* 19: 2888-2894.